Enhancement of the contrast for a hexagonal boron nitride monolayer placed on a silicon nitride/silicon substrate

Hattori, Yoshiaki
Taniguchi, Takashi
Watanabe, Kenji
Kitamura, Masatoshi

(Citation)
Applied Physics Express,15(8):086502

(Issue Date)
2022-08-01

(Resource Type)
journal article

(Version)
Version of Record

(URL)
https://hdl.handle.net/20.500.14094/90009619

Applied Physics Express

LETTER • **OPEN ACCESS**

Enhancement of the contrast for a hexagonal boron nitride monolayer placed on a silicon nitride/silicon substrate

To cite this article: Yoshiaki Hattori *et al* 2022 *Appl. Phys. Express* **15** 086502

OPEN ACCESS

Applied Physics Express 15, 086502 (2022) LETTER

https://doi.org/10.35848/1882-0786/ac8270

Enhancement of the contrast for a hexagonal boron nitride monolayer placed on a silicon nitride/silicon substrate

Yoshiaki Hattori[1*], Takashi Taniguchi[2], Kenji Watanabe[3], and Masatoshi Kitamura[1*]

[1]Department of Electrical and Electronic Engineering, Kobe University, 1-1, Rokkodai-cho, Nada, Kobe 657-8501, Japan
[2]International Center for Materials Nanoarchitectonics, National Institute for Materials Science, 1-1 Namiki, Tsukuba 305-0044, Japan
[3]Research Center for Functional Materials, National Institute for Materials Science, 1-1 Namiki, Tsukuba 305-0044, Japan

*E-mail: hattori@eedept.kobe-u.ac.jp; kitamura@eedept.kobe-u.ac.jp

Received June 21, 2022; revised July 6, 2022; accepted July 18, 2022; published online July 29, 2022

We propose a visualization technique for identifying an exfoliated monolayer hexagonal boron nitride (hBN) flake placed on a SiN_x/Si substrate. The use of a Si substrate with a 63 nm thick SiN_x film enhanced the contrast of monolayer hBN at wavelengths of 480 and 530 nm by up to 12% and −12%, respectively. The maximum contrast for the Si substrate with SiN_x is more than four times as large as that for a Si substrate with a ∼90 or ∼300 nm SiO_2 film. Based on the results of the reflectance spectrum measurement and numerical calculations, the enhancement is discussed.

Supplementary material for this article is available online

Few-layer hBN flakes have been used as a tunneling barrier layer in novel electrical and optical devices[1–3] composed of various two-dimensional (2D) materials. This is due to the atomically flat insulating hBN film's ideal dielectric interface, which efficiently reduces charge scattering[4] and degree of freedom in van der Waals heterostructures.[5,6] Although a monolayer (1L) hBN film has been synthesized by chemical vapor deposition,[7–9] mechanically exfoliated hBN film is still used in fundamental studies because of its high quality.[10,11] When an exfoliated 1L or few-layer hBN film is utilized, it is necessary to find the target hBN fake from films with different thicknesses randomly placed.

In general, a Si substrate with a thermally-grown SiO_2 layer with a thickness of ∼90 or ∼300 nm has been used to visualize 2D materials on the substrate. The SiO_2 thickness contributes to the enhancement of the interference effect in the multilayer structure consisting of the 2D material, SiO_2, and Si layers. In the technique, a 2D material film is identified in a microscopic image by the difference between the reflectance (R) from the 2D material surface and that from the SiO_2 surface. Thus, increasing the difference at a wavelength (λ) improves the optical contrast (C) for the 2D material film in the wavelength observation. However, it has been difficult to visualize a 1L hBN film because of the low contrast. The maximum C at a certain wavelength for a 1L hBN film on a silicon oxide (SiO_2/Si) substrate is ∼2.5%,[12] which is less than ∼10% of monolayer graphene or other 2D transition metal dichalcogenides.[13–15] The low C is caused by the wide bandgap of about ∼6 eV,[16] which results in $k = 0$ in the complex refractive index $N = n - ik$ where n is the refractive index, k is the absorption coefficient, and i is an imaginary unit.

The C of a few-layer hBN film on a substrate observed with an optical microscope can be defined as $(R_{BN}/R_{sub} - 1)$[17,18] where the R_{BN} and R_{sub} are the reflectances from the hBN surface and the substrate surface uncovered with an hBN film, respectively. Thus, it is possible that using a substrate with a low R_{sub} increases the C.[15] As an attempt to enhance the C using a substrate of low R_{sub}, some groups, including ours, have used SiO_2/Si substrates with a structure in which a thin Au layer with a thickness of ∼10 nm is deposited on the ∼90 nm thick SiO_2 layer with a ∼1 nm adhesive layer of Cr,[18] Ti,[19,20] or MoO_x.[17] We successfully identified a few-layer hBN flake placed on a substrate of R_{sub} close to zero at λ of ∼500 nm in the microscope image obtained under a quasi-monochromatic light.[17,18] The C for the 1L hBN was about 4%. In the method, C is sensitive to the thickness of Au. However, the exact thickness control of a thin Au layer is difficult, and such a thin Au layer is mechanically weak. Furthermore, C improvement is still needed to easily find a few-layer hBN flake on a substrate.

In this study, a silicon nitride (SiN_x/Si) substrate is employed instead of a SiO_2/Si substrate for the visualization of a hexagonal boron nitride monolayer. On a SiN_x/Si substrate, no additional layer is required, such as a thin Au layer on a SiO_2/Si substrate. Thus, we can focus on controlling the thickness of the SiN_x layer. In addition, SiN_x is a material used in silicon devices, and it is not difficult to prepare a SiN_x/Si substrate. Although it has been reported that the SiN_x/Si substrate provides an increase in the contrast of graphene and 2D semiconductor layers,[21,22] it is unclear whether a 1L hBN flake is experimentally observed.

The advantage of using SiN_x is based on the refractive index and is explained using an equation for reflectance. When a single homogeneous thin film of $N_1 = n_1 - ik_1$ with a thickness d_1 is deposited on a substrate of $N_2 = n_2 - ik_2$, the reflectance of light vertically incident on the surface from the air, R_{sub}, is given by,[23]

$$R_{sub} = \left| \frac{N_1(N_2 - 1)\cos(2\pi N_1 d_1/\lambda) + i(N_1^2 - N_2)\sin(2\pi N_1 d_1/\lambda)}{N_1(N_2 + 1)\cos(2\pi N_1 d_1/\lambda) + i(N_1^2 + N_2)\sin(2\pi N_1 d_1/\lambda)} \right|^2, \quad (1)$$

where the subscripts of 1 and 2 indicate the thin film and substrate, respectively. When k_1 is zero, the conditions for $R_{sub} = 0$ are

$$n_1^2 = n_2 + \frac{k_2^2}{n_2 - 1}, \tag{2}$$

$$\sin^2\left(\frac{2\pi n_1 d_1}{\lambda}\right) = \frac{n_1^2}{n_1^2 - 1}\frac{n_2 - 1}{n_2}. \tag{3}$$

The two equations determine the values of n_1 and d_1 under the condition that R_{sub} equals zero at a certain λ. In Fig. 1(a), the solid and dashed black lines show n_1 and d_1 values calculated from Eqs. (2) and (3) as a function of λ for a Si substrate, respectively. The green line shows the refractive index of the Si substrate, n_2. Since k_2 of Si is small in the visible light range, n_1 is close to $\sqrt{n_2}$.[24] The red and light blue lines show the refractive indices of SiN_x and SiO_2, respectively. SiN_x and SiO_2, which are typical transparent materials, have k that nearly equals zero in the visible light range.[25,26] The n of SiN_x is close to the ideal n in the wide wavelength range compared with that of SiO_2. Thus, it is expected to realize low R_{sub} using a SiN_x layer. Figure 1(b) shows the R_{sub} of the SiN_x/Si substrate calculated as a function of d_1 and λ for vertically incident light. The dark area expresses low R_{sub}. The SiN_x thickness that R_{sub} is minimum at a λ gradually increases from 50 to 80 nm. The minimum R_{sub} is close to zero and is less than 0.5%.

The reflectance spectra of SiN_x/Si and SiO_2/Si substrates were measured using an optical microscope (LV100, Nikon) equipped with a spectroscope (BTC-110S, B&W Tek) at the trinocular head for experimental verification. The experiment used Si substrates with a 150 nm thick SiN_x (Fuleda Technology) and a 94 nm thick (Furuuchi Chemical). The substrates were cleaned by sonication in acetone and 2-propanol for each 5 min. For adjusting the thickness of the SiN_x layer to ~70 nm, the SiN_x surface was etched at room temperature for several hours in solution obtained by diluting 48wt% HF solution (FUJIFILM Wako Pure Chemical Co.) with nine times the volume of deionized water. Without etching, the SiO_2/Si substrate was used. The thicknesses of the SiN_x and SiO_2 layers were determined based on spectra obtained by ellipsometry (Auto SE, Horiba) and/or reflectance spectroscopy measurement. Typical root-mean-square roughnesses of the SiN_x and SiO_2 layers measured by an atomic force microscope (AFM, NanoNavi; SII, Japan) are 0.4 and 0.2 nm, respectively. The solid lines in Fig. 2(a) represent reflectance spectra measured through an objective lens with a numerical aperture (NA) of 0.15 (LU Plan Fluor 5×/0.15, Nikon) for SiO_2/Si and SiN_x/Si substrates with d_1 values indicated in the figure. For comparison, the reflectance was calculated using the transfer matrix method, taking into account the oblique incidence.[27,28] The calculation results represented by dashed lines roughly reproduce the experiment represented by solid lines. For SiN_x/Si substrates, the R_{sub} spectra for $d_1 = 66$ nm and 73 nm have values close to zero around $\lambda = 550$ nm and 600 nm, respectively. While the R_{sub} spectrum for the SiO_2/Si substrate has a minimum of about 10% at $\lambda = 570$ nm.

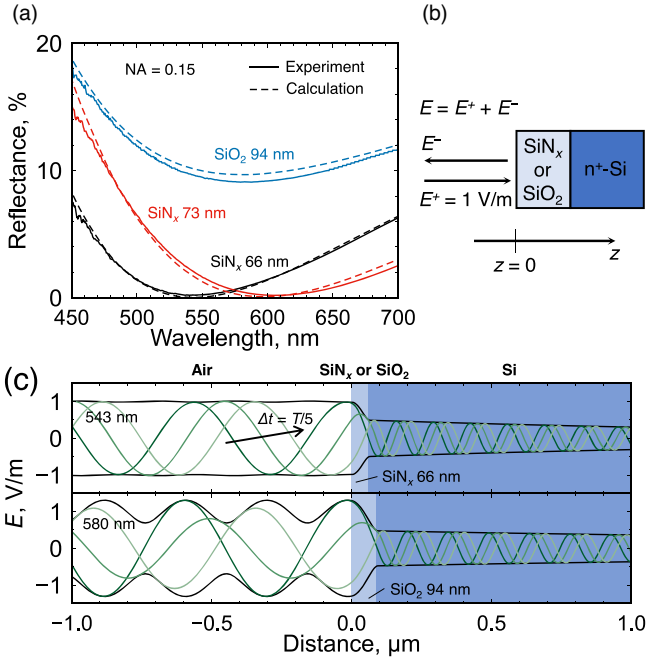

Fig. 2. (Color online) (a) Experimental and calculated reflectance spectrum measured through an objective lens of NA = 0.15 for SiO_2/Si and SiN_x/Si substrates with different thickness films. (b) Model for the calculation of electromagnetic waves. (c) The propagation of electromagnetic waves for SiO_2/Si and SiN_x/Si substrate at the minimum reflection. The upper and lower graphs are for 66 nm SiN_x at 543 nm and 94 nm SiO_2 at 580 nm, respectively. The black solid lines represent the standing wave pattern. The standing wave is generated from the incident and reflected waves only in the SiO_2/Si substrate.

Electromagnetic waves incident on a substrate with a multilayer structure can be calculated analytically. To examine the propagation of electromagnetic waves on the reflectance, we calculated the electric field for the model

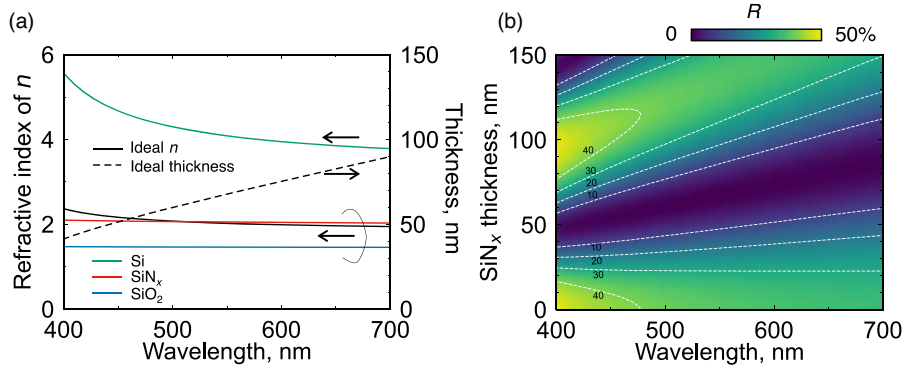

Fig. 1. (Color online) (a) The n_1 and d_1 of a single layer film with $k_1 = 0$ on a Si substrate under the condition that R_{sub} equals zero. The black solid and dashed lines indicate the n_1 and d_1, respectively. The n of SiN_x is close to the ideal n in the wide wavelength range as compared to that of SiO_2. (b) The reflectance of the SiN_x/Si substrate is calculated as a function of the d_1 and λ for vertically incident light.

shown in Fig. 2(b). In the calculation, the amplitude of the electric field was set to 1 V m^{-1}. The green solid lines in Fig. 2(c) show the electric field at a time calculated for substrates with 66 nm SiN_x at $\lambda = 543$ nm and with 94 nm SiO_2 at $\lambda = 580$ nm. T in the figure is the period. The standing wave pattern is indicated by the solid lines, which correspond to the envelope of electric field waveforms at a given time. For the SiN_x/substrate, the standing wave in the air region is a constant of ~1 V m^{-1}, and is generated from the incident wave. This means matching optically without reflected light. While, for the SiO_2/Si substrate, the standing wave is generated from the incident and reflected waves.

The optical contrast of a few-layer hBN on a substrate was investigated based on calculation. Figure 3(a) shows the calculation model. In the calculation of the reflectance of the substrate with hBN, and R_{BN}, the refractive index and thickness of the hBN are set up to $2.2 - i0$ and $l \times 0.333$ nm,[12] respectively. Here l is the layer number. Figures 3(b) and 3(c) show the contrast of a 1L hBN calculated as a function of λ and d_1 for SiN_x/Si and SiO_2/Si substrates, respectively. The color bar in Fig. 3(b) is adapted for both figures. A SiN_x/Si substrate with a thickness in the range of 50–80 nm provides a high contrast at a certain λ. However, the contrast of the SiO_2/Si substrate is low even if the wavelength is adjusted. The SiN_x/Si substrate result suggests that exact control of SiN_x thickness is not needed. The high contrast can be realized by selecting an appropriate λ. These characteristics are also applied for few-layer hBN flakes or ~300 nm SiO_2 film [see Figs. S1 and S2 in supplementary data (available online at stacks.iop.org/APEX/15/086502/mmedia)].

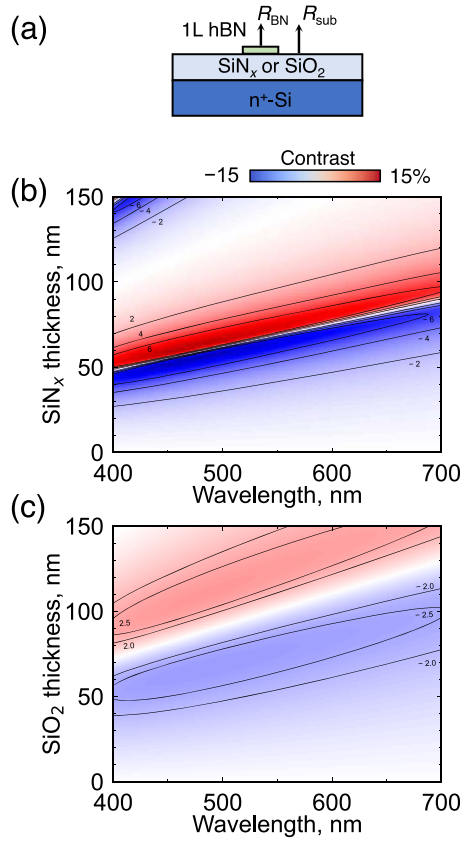

Fig. 3. (Color online) (a) Model for the calculation of C. (b) and (c) calculated contrast of 1L hBN on a SiN_x (b) and SiO_2 (c) film as a function of λ and d_1 for NA = 0.75. The color bar in (b) is adapted for both figures, indicating the enhancement of the contrast by the SiN_x/Si substrate.

For experimental verification, the contrast of exfoliated few-layer hBN films on a Si substrate with a 63 nm thick SiN_x was measured. The hBN films were photographed in an optical microscope equipped with an objective lens with a NA of 0.8 (LU Plan Fluor 50×/0.80, Nikon) using a color 8-bit camera (EOS Kiss X4, Canon) or a monochrome 12-bit camera (CS-63M, Bitran) cooled down to 10 °C at ~25 °C in the air with a relative humidity of 30%–40%. A narrow band-pass filter was inserted just after the collector lens for the halogen lamp in the optical path of the microscope. As a normal value, the full width at half-maximum of the narrow band-pass filters for imaging is 10 nm. The angle of incidence in the objective was restricted by the aperture stop to ~90% of the objective's NA. Figures 4(a) and 4(b) show a 1L hBN flake observed with and without a narrow band-pass filter at 480 nm, respectively. Figure 4(a) is an image obtained without image processing software. The use of an appropriate narrow band-pass filter provides the image with high contrast for a 1L hBN flake. However, Fig. 4(b) is an image where the contrast is enhanced by image processing. Although not using a filter decreases the contrast, image processing contributes to finding a 1L hBN flake. The result suggests that we can find a 1L or a few-layer hBN flake without an optical filter from a large number of thick hBN films. Figure 4(c) shows a height AFM image corresponding to the dotted area in Fig. 4(a). Figure 4(d) shows the average height profile along the white solid bold line in Fig. 4(c). The average area is indicated by the vertical short dashed lines at both ends of the bold line. The height step of ~0.5 nm corresponds to the thickness of a 1L hBN film.[29–31] Similar data for few-layer hBN flakes are described in Figs. S3 and S4 in supplementary data.

The wavelength-dependent contrast was investigated quantitatively by a monochrome camera with a band-pass filter for various λ. The solid lines in Fig. 5(a) represent the experimental contrast spectra for 1 and 2L hBN films on a SiN_x film with a thickness of 63 nm. The dashed lines in the figure represent spectra calculated by assuming NA = 0.75. The calculated spectra roughly reproduce the experiment. For both 1 and 2L hBN films, the contrast is high at around 480 and 530 nm. The maximum contrast of 12% at 480 nm for 1L hBN is comparable to that of a 1L graphene on a 90 nm SiO_2 film.[13] Figure 5(b) shows the contrast of 1−4L hBN at 480 nm. The experimental and calculated contrasts are represented by solid and dashed lines, respectively. The contrast increases with the number of layers. This result can be used for the determination of a layer number. For comparison, the contrast calculated for hBN layers on SiO_2 film with a thickness of 94 nm is shown as a light-red dashed line in the figure. The contrast of 1L hBN on the SiN_x/Si substrate is more than four times as large as that on the Si/SiO_2 substrate. The thickness of 94 nm is optimized. Note that the calculations of SiO_2 in the study for 1 and 2L hBN are roughly in agreement with the past literature values.[12]

In summary, the reflectance of a SiN_x/Si substrate was investigated by experiment and calculation. At a certain wavelength, the reflectance nearly equals 0%. This is because the refractive index of SiN_x optically matches that of Si, which was explained by the analytical solution. A thin film

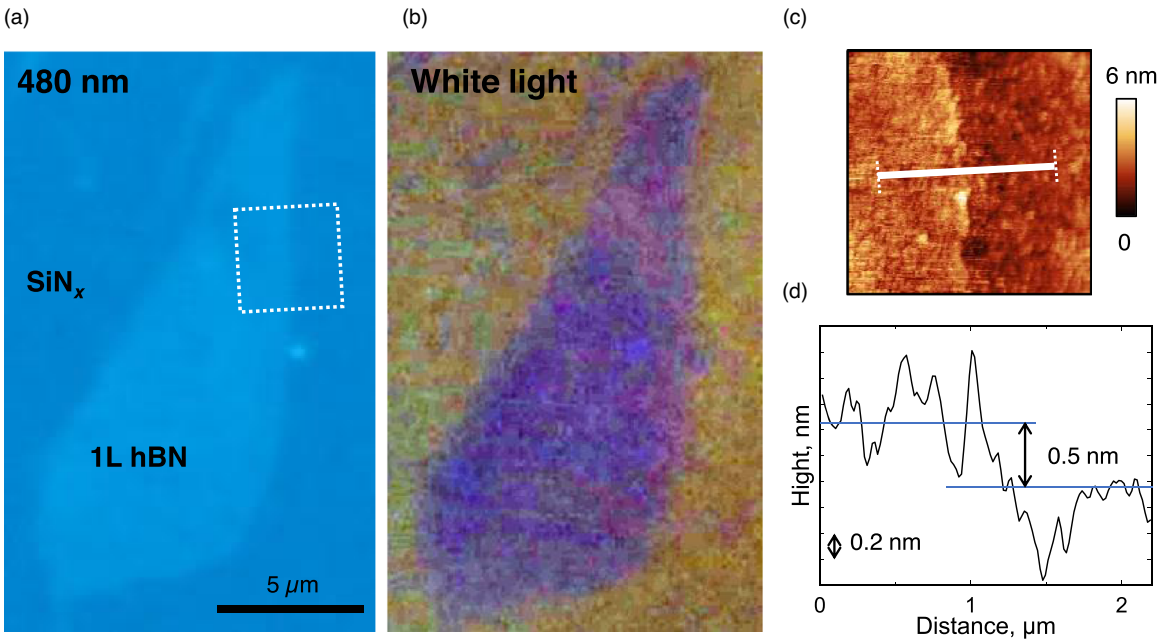

Fig. 4. (Color online) Observation of 1L hBN on 63 nm SiN_x film. (a) and (b) Photograph was taken with and without a narrow band-pass filter for 480 nm, respectively. The image of (a) has not been applied by image processing. While the contrast of the image of (b) is strongly enhanced by image processing. (c) Height AFM image corresponds to the dotted area in (a). (d) A profile of average height along the white solid bold line in (c).

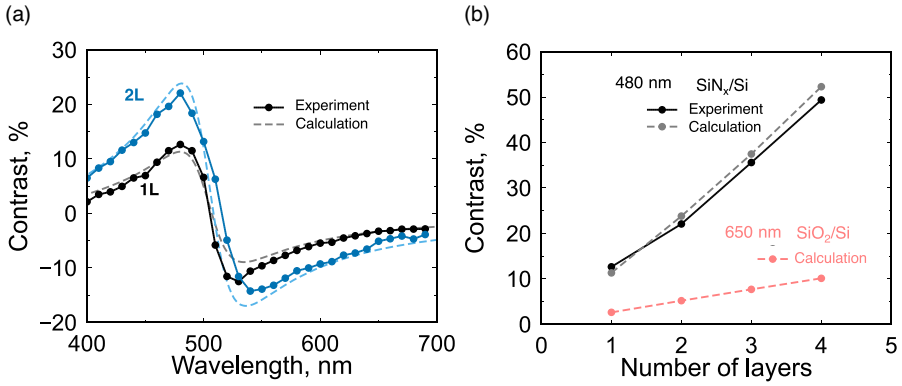

Fig. 5. (Color online) Contrast of 1L and few-layer hBN on SiN_x/Si substrate measured through an objective lens of NA = 0.80. The NA for the calculation is assumed to be 0.75. (a) Contrast spectra for 1 and 2L hBN. (b) The contrast depends on the number of hBN layers at 480 nm. In both figures, the solid and dashed lines indicate the experiment and calculation, respectively. The light-red dashed line in (b) is for the 94 nm SiO_2 film for comparison.

placed on the SiN_x/Si substrate changes the reflectance spectra slightly. Therefore, the presence of the thin film is recognized in a microscopic image because of the different reflectance from that of the SiN_x/Si surface. Experimentally, the wavelength-dependent contrast of an exfoliated 1L hBN film on a 63 nm SiN_x film was measured with various band-pass filters. The contrast increases up to 12% and −12% at 480 and 530 nm, respectively. The contrast is consistent with that obtained from a multilayer model. The maximum contrast of 1L hBN on the SiN_x/Si substrate is more than four times as large as that on the optimized Si/SiO_2 substrate that has been generally used. Since the enhancement effect also affects observation under white light, 1L hBN can be seen even without a band-pass filter. The observation is useful in practical applications. Furthermore, the number of layers of hBN can be determined from the linearity of the contrast.

Acknowledgments This work was partly supported by a JSPS KAKENHI Grant Nos. 21K04195, 21H04655, Kansai Research Foundation, Chubei Itoh Foundation, Iketani Science and Technology Foundation, and Hyogo Science and Technology Association.

Notes

The authors declare no competing financial interests.

ORCID iDs Yoshiaki Hattori https://orcid.org/0000-0002-5400-8820

1) J. Wang et al., Adv. Mater. **28**, 8302 (2016).
2) X. Cui et al., Nano Lett. **17**, 4781 (2017).
3) F. Withers et al., Nano Lett. **15**, 8223 (2015).
4) C. R. Dean et al., Nat. Nanotech. **5**, 722 (2010).
5) L. Britnell et al., Nano Lett. **12**, 1707 (2012).
6) M. Vizner Stern, Y. Waschitz, W. Cao, I. Nevo, K. Watanabe, T. Taniguchi, E. Sela, M. Urbakh, O. Hod, and M. Ben Shalom, Science **372**, 1462 (2021).
7) T.-A. Chen et al., Nature **579**, 219 (2020).
8) G. Kim, A.-R. Jang, H. Y. Jeong, Z. Lee, D. J. Kang, and H. S. Shin, Nano Lett. **13**, 1834 (2013).
9) J.-H. Park et al., ACS Nano **8**, 8520 (2014).
10) D. Wong et al., Nat. Nanotech. **10**, 949 (2015).
11) Y. Hattori, T. Taniguchi, K. Watanabe, and K. Nagashio, ACS Appl. Mater. Interfaces **8**, 27877 (2016).
12) R. V. Gorbachev et al., Small **7**, 465 (2011).

13) P. Blake, E. W. Hill, A. H. Castro Neto, K. S. Novoselov, D. Jiang, R. Yang, T. J. Booth, and A. K. Geim, Appl. Phys. Lett. **91**, 063124 (2007).
14) A. Castellanos-Gomez, N. Agraït, and G. Rubio-Bollinger, Appl. Phys. Lett. **96**, 213116 (2010).
15) F. Huang, J. Phys. Chem. C **123**, 7440 (2019).
16) G. Cassabois, P. Valvin, and B. Gil, Nat. Photon. **10**, 262 (2016).
17) Y. Hattori, H. Takahashi, N. Ikematsu, and M. Kitamura, J. Phys. Chem. C **125**, 14991 (2021).
18) Y. Hattori, T. Taniguchi, K. Watanabe, and M. Kitamura, Nanotechnology **33**, 065702 (2021).
19) M. Velický et al., ACS Nano **12**, 10463 (2018).
20) G. E. Donnelly, M. Velický, W. R. Hendren, R. M. Bowman, and F. Huang, Nanotechnology **31**, 145706 (2020).
21) G. Rubio-Bollinger, R. Guerrero, D. P. De Lara, J. Quereda, L. Vaquero-Garzon, N. Agraït, R. Bratschitsch, and A. Castellanos-Gomez, Electronics **4**, 847 (2015).
22) J. Y. An and Y. H. Kahng, AIP Adv. **8**, 015107 (2018).
23) A. Musset and A. Thelen, in *Progress in Optics*, ed. E. Wolf (Elsevier, Amsterdam, 1970) Vol. 8, p. 201.
24) D. F. Edwards, in *Handbook of Optical Constants of Solids*, ed. E. D. Palik (Academic, New York, 1998), p. 547.
25) I. H. Malitson, J. Opt. Soc. Am. **55**, 1205 (1965).
26) K. Luke, Y. Okawachi, M. R. E. Lamont, A. L. Gaeta, and M. Lipson, Opt. Lett. **40**, 4823 (2015).
27) Y. Lu, X.-L. Li, X. Zhang, J.-B. Wu, and P.-H. Tan, Sci. Bull. **60**, 806 (2015).
28) C. Casiraghi, A. Hartschuh, E. Lidorikis, H. Qian, H. Harutyunyan, T. Gokus, K. S. Novoselov, and A. C. Ferrari, Nano Lett. **7**, 2711 (2007).
29) Y. Li, Z. Cui, Y. He, H. Tian, T. Yang, C. Shou, and J. Liu, Appl. Phys. Lett. **120**, 173104 (2022).
30) L. H. Li, J. Cervenka, K. Watanabe, T. Taniguchi, and Y. Chen, ACS Nano **8**, 1457 (2014).
31) Y. Gao, W. Ren, T. Ma, Z. Liu, Y. Zhang, W.-B. Liu, L.-P. Ma, X. Ma, and H.-M. Cheng, ACS Nano **7**, 5199 (2013).